RADC-TDR-63-508

DEVELOPMENT OF ADVANCED MICROWAVE COMPONENTS AND TECHNIQUES - PLANAR HEXAGONAL FERRITES AND DEVICES.

TECHNICAL DOCUMENTARY REPORT NO. RADC-TDR-63-508

December 1963

Techniques Branch
Rome Air Development Center
Research and Technology Division
Air Force Systems Command
Griffiss Air Force Base, New York

Project No. 4506, Task No. 450602

(Prepared under Contract No. AF30(602)-2757 by Sperry Microwave Elecrronics Company, Clearwater, Florida.)

Key Words: Ferrites, hexagonal; microwave, advanced components.

ABSTRACT

Studies have been made of the preparation and properties of Y compounds with compositions near $Zn_{2.0}Y$, $Ni_{1.0}Zn_{1.0}Y$, $Cu_{0.5}Zn_{1.5}Y$, and $Ni_{0.3}Cu_{0.7}Zn_{1.0}Y$. X-ray diffraction patterns taken on Y compounds with aluminum substituted for iron strongly indicate the formation of a second phase, rather than a replacement of Fe^{+3} by Al^{+3} in the Y structure. While densities of greater than 95 percent of the theoretical value and alignment indices of 0.98 and above have been obtained, linewidths remain somewhat high, approximately 400 oersteds. Attempts at preparing Y compounds from topotactical reaction of M compounds and raw oxides have proved fruitless, and with firing temperatures up to 1400°C no reaction occurs.

Because of the extremely good alignment of planar materials achieved, experiments have been started to orient cubic materials. Initial experiments with polycrystalline yttrium iron garnet have been very encouraging, and linewidths of 18 to 19 oersteds have been obtained.

Initial investigation of the application of planar ferrites to isolator structures are reported. Because of the small sizes and shapes of planar ferrites now available only low isolation values are found, but isolation ratios of as high as 60 are obtained.

PUBLICATION REVIEW

This report has been reviewed and is approved. For further technical information on this project, contact EMATE, JOSEPH M. SCHENNA, X4251

Approved: Joseph M. Schenna
JOSEPH M. SCHENNA
Project Engineer
Electron Devices Section
Techniques Branch

Approved: Paul H. Baldwin
for Lt Col USAF
ARTHUR J. FROHLICH, Chief
Techniques Branch
Surveillance and Control Division

AIR FORCE, Cato Show Prtg. Co. 1 15 64 138

TABLE OF CONTENTS

ADVANCED MICROWAVE COMPONENTS AND TECHNIQUES PLANAR HEXAGONAL FERRITES AND DEVICES

1. INTRODUCTION

This report covers work performed under Contract AF30(602)-2757 FSC-A082, Development of Advanced Microwave Components and Techniques - Planar Hexagonal Ferrites and Devices, for the period from June 28, 1963 to September 28, 1963. This report describes and discusses continued progress in the first, or materials, phase of the program and initial experiments on the second, or applications, phase.

The results reported show that the materials synthesis efforts have produced materials of good ceramic quality with high densities and extremely high alignment factors. In view of these favorable indications it is somewhat surprising that linewidths no more narrow than 375 oersteds have been obtained. Attempts are being made to reconcile this data.

Because of the extremely good alignment obtained in planar materials, it was felt justified to attempt orientation of cubic ferrites. Preliminary, but very encouraging results are reported that could have very significant practical importance.

The initial isolator structure measurements reported should be considered in view of the fact that only small samples of a single material were used, and therefore these results represent only preliminary findings.

2. OBJECT

The object of this project is to investigate theoretically and experimentally the microwave characteristics of planar hexagonal magnetic oxides, with emphasis on their application to microwave devices and circuits.

Particular emphasis shall be placed on the development of a series of planar magnetic materials whose magnetization, anisotropy field, and linewidth can be controlled over a range of values suitable to microwave application. Efforts shall be directed towards the utilization of these materials in low frequency (1.0 Gc to 10 Gc) devices.

One goal of this program is to demonstrate the effectiveness of hexagonal magnetic materials towards the reduction of magnet size in low frequency resonance isolators. A study will also be made of techniques of using planar materials in microwave switches to reduce the external switching field required and, for a given switching field, to increase the switching speed.

3. PROGRESS OF PROJECT

3.1 MATERIAL SELECTION

During this second quarter of the program more complete data have been obtained on material properties as a function of firing temperature for a number of compositions. Five different compositions have been studied with rather complete firing curves obtained for three of these.

For isolator applications it is well known intuitively and demonstrated analytically in Section 3.5 that best results will be obtained on materials having the narrowest resonance linewidth and the lowest dielectric loss. The field of materials suitable for this application can be narrowed down to compositions near $Ni_{.3}Cu_{.7}Zn_{1.0}Y$, $Ni_{1.0}Zn_{1.0}Y$, or $Cu_{.5}Zn_{1.5}Y$. The optimum compositions probably lie near one of these compositions.

At this point it is not yet clear what material characteristics are most important for the switching application, and therefore some of the more highly anisotropic compositions like $Co_{2/3}Cu_{2/3}Zn_{2/3}Y$ will continue to be investigated.

The substitution of aluminum for iron, initiated in the last quarter, was found to be fruitless for controlling the magnetization of the material. X-ray data indicated that the aluminum substitution resulted in a second phase formation in the material that adversely affected its microwave properties. This family of materials has therefore been dropped.

3.2 SYNTHESIS TECHNIQUES

The preparation process used in this quarter was essentially the same as that outlined in the First Quarterly Report. Experimental data obtained on a variety of samples indicate that the use of ethyl alcohol as the carrier in the attritoring

stage results in better material properties and greatly facilitates the pressing process.

The topotactical reaction technique discussed in the last Quarterly Report failed to give sufficiently encouraging results to warrant continuance. Firing temperature as high as 1400°C failed to produce a conclusive conversion of the M compound plus raw oxides to the desired Y structure.

3.3 MEASUREMENTS

The measurement techniques discussed in the First Quarterly Report have not been altered with the exception of the determination of resonance properties. Resonance measurements have been carried out in cavities at both X-band (9300 Mc) and V-band (37000 Mc) frequencies. The use of two frequencies allows the calculation of the anisotropy field and g-factor without having to resonate the material with the d-c field applied in the hard direction. A free mounted sphere can then be used in both cavities. For each frequency Kittel's equation then takes the familiar form for resonance of a planar material with d-c magnetic field applied in the easy plane

$$\omega_1 = \gamma\left[H_{01}(H_{01} + H_A)\right]^{\frac{1}{2}} \tag{1}$$

where H_{01} is the applied d-c field required for resonance at the frequency ω_1, and H_{anis} is the effective planar anisotropy field of the material. Since a spherical sample is used the demagnetizing terms do not enter this equation. A similar equation will hold for frequency ω_2, and the anisotropy field may then be calculated by taking the ratio

$$\frac{\omega_1}{\omega_2} = \left\{\frac{(H_{01} + H_A)(H_{01})}{(H_{02} + H_A)(H_{02})}\right\}^{\frac{1}{2}} \tag{2}$$

and therefore $H_A = \dfrac{H_{01}^{2} - \left(\dfrac{\omega_1}{\omega_2}\right)^2 H_{02}^{2}}{\left(\dfrac{\omega_1}{\omega_2}\right)^2 H_{02} - H_{01}}$.

The gyromagnetic factor γ can then be calculated from equation (1) using the results of (2). In these calculations the assumption is made that H_A and γ are the same at the two frequencies used.

In these measurements the d-c magnetic field is applied in the easy plane, but the r-f magnetic field has no definite orientation with respect to this plane. The question has arisen as to whether or not the measured linewidth would vary with orientation of the r-f field also. Such a dependence would explain some of the observed variation of linewidth on a given composition. To resolve this question measurements are planned for the next quarter with h_{rf} applied both in the easy plane and at right angles to this plane.

3.4 RESULTS

Measured values of density and alignment factor for materials fired at various temperatures are shown in Figures 1 through 6. The first three figures show complete sets of data on the Zn_2Y, the $Cu_{.5}Zn_{1.5}Y$, and the $Ni_{.3}Cu_{.7}Zn_{1.0}Y$ materials for batches in which alcohol, water, and Nyso 45 were used as carriers in the attritor stage of the preparation process. Figures 4, 5, and 6 show similar though somewhat less complete data. In particular, the compositions $Ni_{1.0}Zn_{1.0}Y$ and $Co_{2/3}Cu_{2/3}Zn_{2/3}$ shown in Figures 5 and 6 respectively have not yet been prepared using alcohol as the carrier.

Figure 1 shows that the density of the Zn_2Y composition is not greatly affected by the type of carrier used. Equally good results were obtained with either the alcohol or Nyso 45 carriers. The solid line of this graph represents a calculated theoretical density based on the lattice constants for the Y compounds and the molecular weights of the constituent ions. [illegible] in density which occurs [illegible]

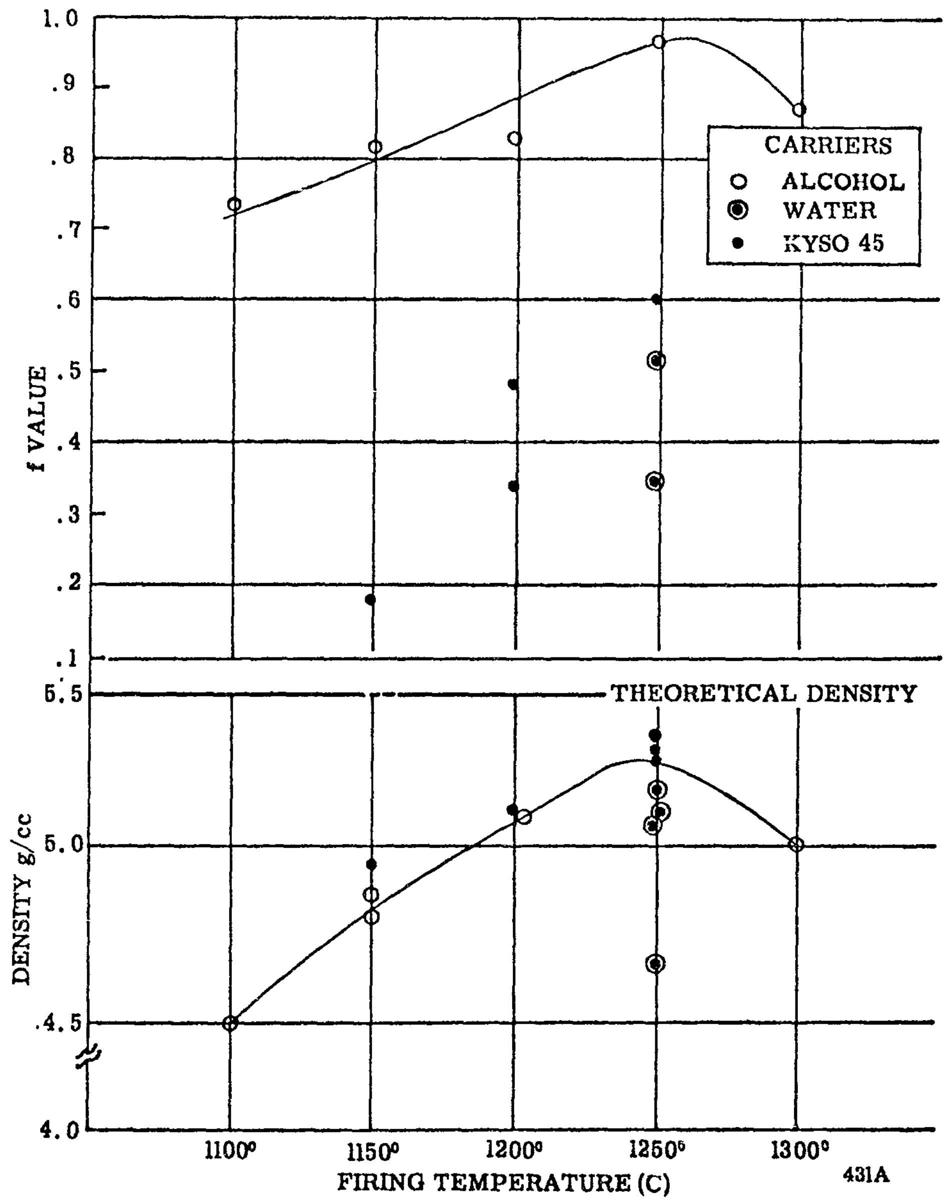

Figure 1. Density and alignment index of Zn_2Y samples plotted as a function of firing temperature. Data are shown for three different carriers used in the attritoring process.

REFERENCES

1. B. Lax and K. J. Button, Microwave Ferrites and Ferrimagnetics, McGraw Hill Book Co., Inc., New York, N.Y., 1962, p. 575.

2. I. Bady, IRE Trans MTT-9, 52, (1961).

6. PERSONNEL

During the second quarter, time spent on the project by technical personnel was as follows:

ENGINEERING PERSONNEL	
J. E. Pippin	28 hours
G. P. Rodrigue	85 hours
H. A. Willing	405 hours
Total Engineering Time	518
LABORATORY TECHNICIANS	604 hours
SHOP PERSONNEL	149 hours
TOTAL	1271

In this same period the following time was spent on company sponsored, directly related research:

ENGINEERING PERSONNEL	
J. E. Pippin	37 hours
G. P. Rodrigue	83 hours
E. L. Meeks	90 hours
Total Engineering Time	210
LABORATORY TECHNICIANS	8 hours
GRAND TOTAL	1489 hours

density that is 96.5 percent of the theoretical density. The alignment factor data given at the top of this graph shows a decided improvement in alignment factor when alcohol is used as the carrier in the attritor stage. A firing temperature of 1250°C was also found to produce a maximum alignment factor of .97. This very marked improvement in alignment with the use of alcohol as the carrier has been consistently found for all materials prepared. While 1250°C would be an optimum firing temperature for this Zn_2Y material as far as density and alignment are concerned, the actual firing temperature will be influenced also for practical materials by the affect of firing temperature on dielectric loss tangent. (See Figures 7 and 8 and accompanying discussion.)

Figure 2 shows curves of density and f-factor for the $Cu_{.5}Zn_{1.5}Y$ materials as a function of firing temperature. For this material a substantial improvement in alignment is again noted on these samples in which alcohol was used as the carrier. For this particular material the maximum density of the samples attritorized with alcohol was reached at a decidedly lower firing temperature than was the case for samples prepared using either water or Kyso 45 in the attritoring stage. For this material polyvinyl alcohol wax was used as a binder with the Kyso 45. The maximum density obtained at 1150°C represents 97 percent of the theoretical density calculated from X-ray data and the molecular weights of the constituent ions. The alignment index data shown in the upper portion of this graph show a maximum value achieved at 1200°C or above. An optimum firing temperature might lie between 1150°C and 1200°C depending on the dielectric loss variation with firing temperature. The maximum alignment index for this material was very nearly .99 and represents essentially complete alignment of the grains within the polycrystalline material.

Similar data on the $Ni_{.3}Cu_{.7}Zn_{1.0}Y$ material are shown in Figure 3. This material was not prepared with Kyso 45 as a carrier, hence only the curve for alcohol and a few points for water are shown. The maximum density is achieved for

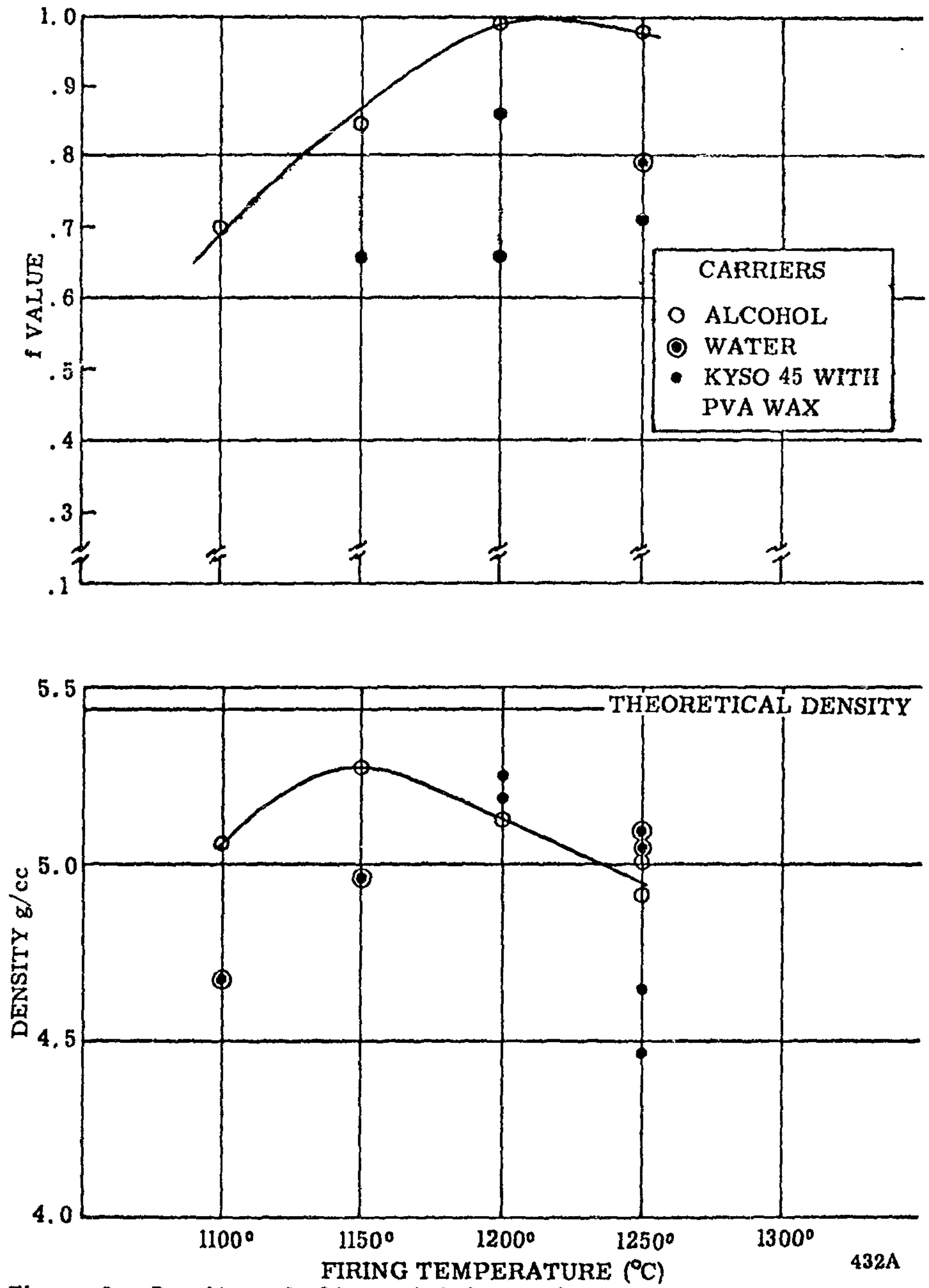

Figure 2. Density and alignment index of $Cu_{0.5}Zn_{1.5}Y$ samples plotted as a function of firing temperature. Data are shown for three different carriers used in the attritoring process.

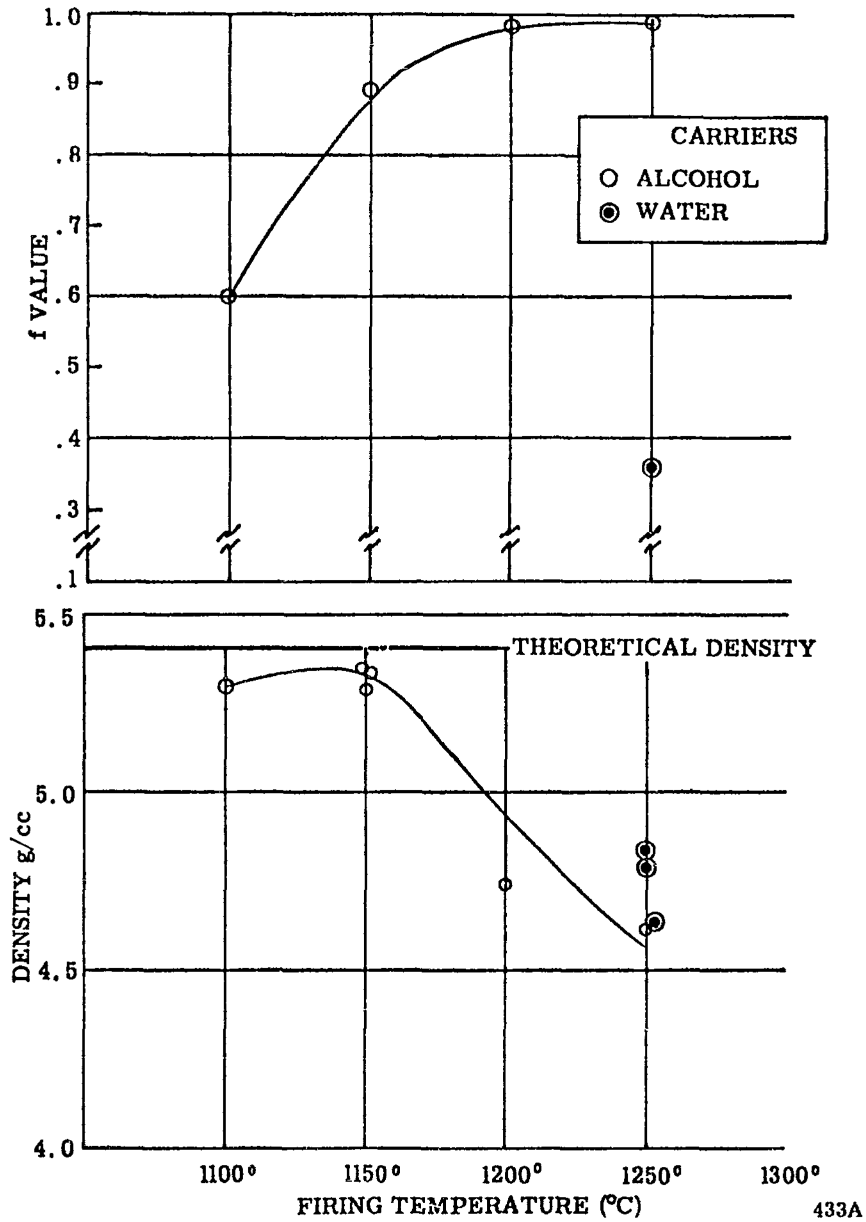

Figure 3. Density of alignment index of $Ni_{0.3}Cu_{0.7}Zn_{1.0}Y$ samples plotted as a function of firing temperature. Data are shown for two different carriers used in the attritoring process.

a firing temperature near 1150°C and represents 98 percent of the theoretical density. The maximum alignment once again occurs for higher firing temperatures - at 1200°C and above. A very marked improvement is noticed in these curves when alcohol is used in the attritor stage. Once again an optimum firing temperature should be determined by considering the temperature necessary to achieve high density, good alignment, and low dielectric loss.

Figure 4 shows density and alignment indices for three different materials having the basic $Ni_{.3}Cu_{.7}Zn_{1.0}Y$ composition with various amounts of aluminum substituted for the iron. While this substitution was initiated in an attempt to control the magnetization of this material, the effort has been abandoned because of the results evidenced here. The upper portion of this curve shows that the alignment index is greatly deteriorated upon the substitution of aluminum for iron. Taking, as an example, the firing temperature of 1250°C we find that in two batches of materials prepared using alcohol as the carrier, the alignment index drops from approximately .99 to .7 upon the substitution of 5 percent aluminum for iron. For the same substitution and with the firing temperature of 1200°C the alignment index drops from .98 to less than .2. The observed X-ray diffraction patterns strongly indicate that the aluminum does not actually replace iron in the Y structure but instead goes into a second phase in the material. Such second phase formation is evidenced by a drastic decrease in indicated alignment factor. This evidence, together with that obtained on magnetization for these aluminum substituted materials, was taken as sufficiently conclusive to eliminate such compositions from further consideration.

Figures 5 and 6 show data taken on two further compositions that have not yet been prepared using alcohol as the carrier. In both cases the alignment factor

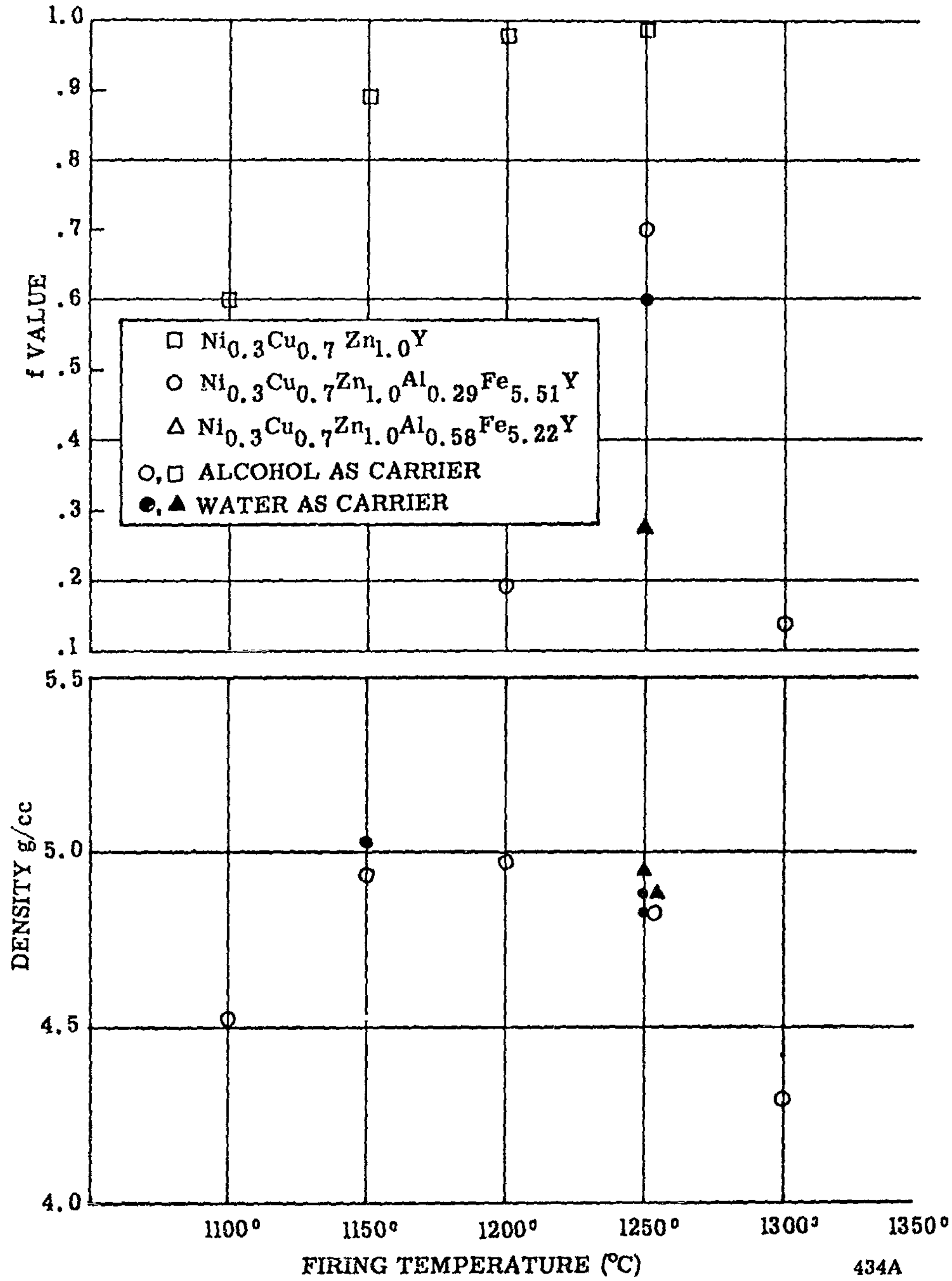

Figure 4. Density and alignment plotted as a function of firing temperature for $Ni_{0.3}Cu_{0.7}Zn_{1.0}Y$ compounds in which there has been a partial substitution of aluminum for iron. Data are shown for two different carriers used in the attritoring process.

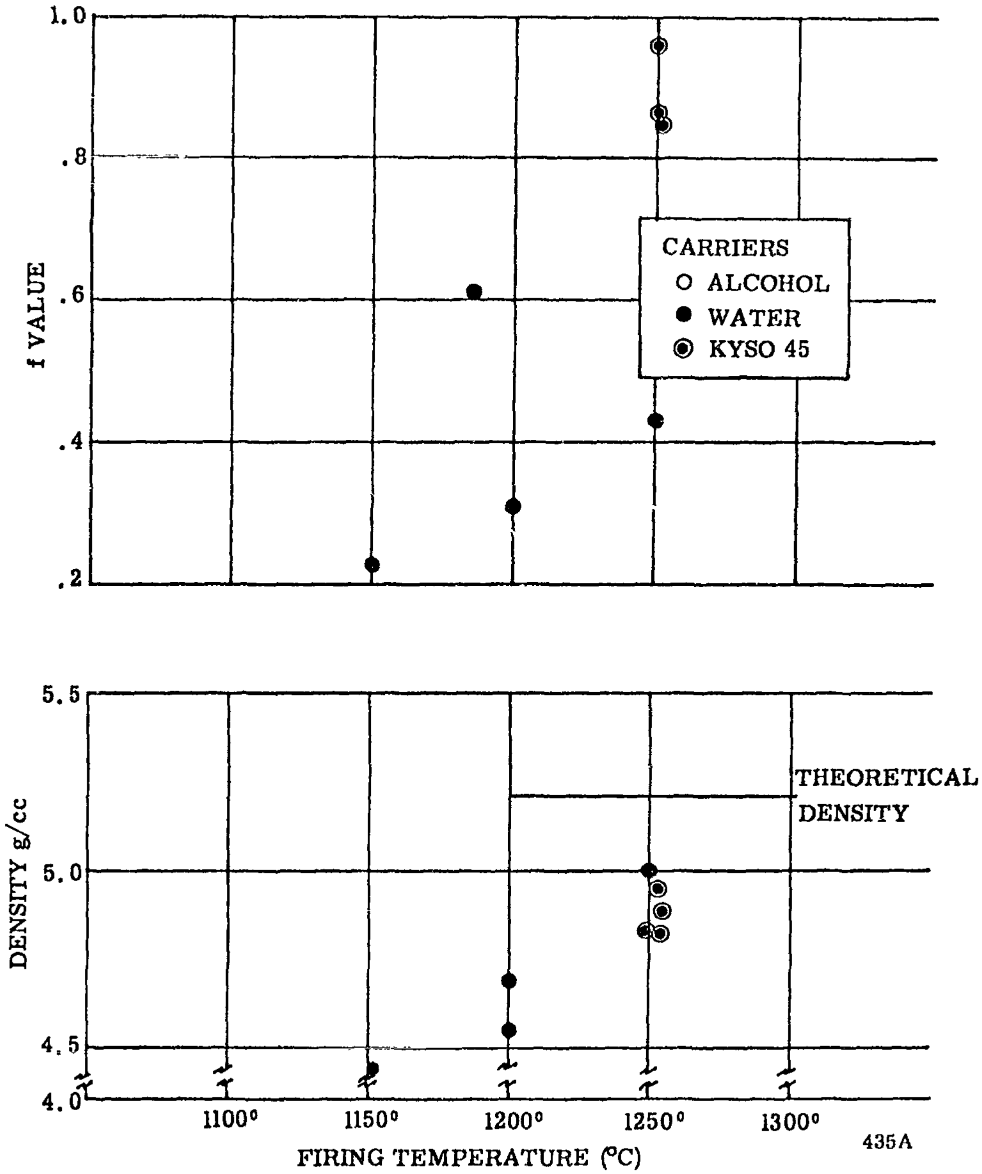

Figure 5. Density and alignment index for $Ni_{1.0}Zn_{1.0}Y$ samples plotted as a function of firing temperature. Data are shown for two different carriers used in the attritoring process.

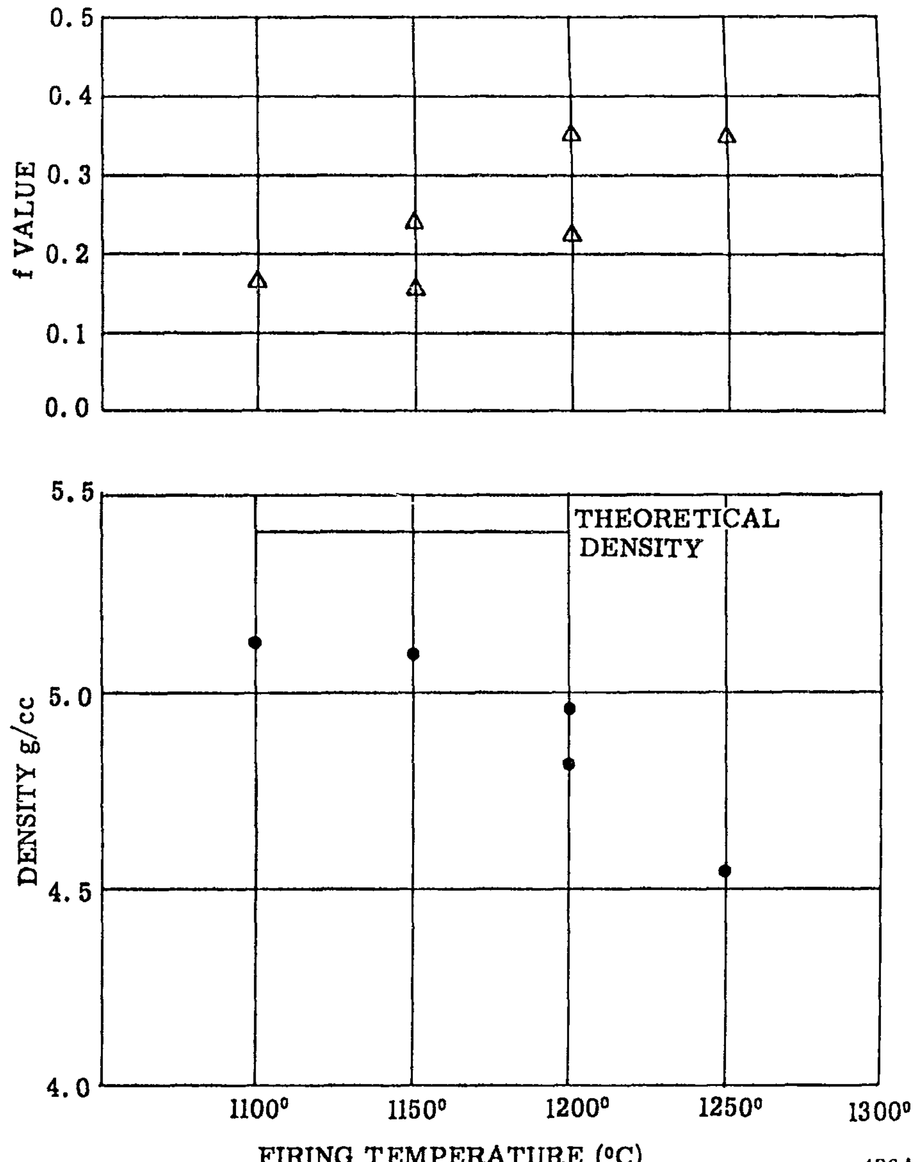

Figure 6. Density and alignment index for $Co_{2/3}Cu_{2/3}Zn_{2/3}Y$ samples plotted as a function of firing temperature. All data shown were obtained with Kyso 45 as the carrier in the attritoring process.

is inferior to the general run of materials, and it is expected that considerably improved results will be obtained when these materials are prepared with the alcohol carrier.

Data on dielectric loss tangent as a function of firing temperature for the $Zn_{2.0}Y$ material are shown in Figures 7 and 8. Three compositions with different iron content were tried. The starting compositions of these three compounds were varied from approximately 3 percent iron deficient (5.8 Fe) to approximately 6-1/2 percent iron deficient (5.6 Fe), to 10 percent iron deficient (5.4 Fe). Figure 7 shows data taken in an X-band cavity on rods of the material 40 mils in diameter, while Figure 8 represents data taken on discs of the material at 20 Mc using a Boonton Q meter. It is felt that for microwave purposes the X-band cavity perturbation measurements are considerably more reliable than are the Q meter measurements. In general, the measured data are in reasonably good agreement. There is a considerable spread in the Q meter measurements, but this is inherent in the accuracy of the measurement. It is seen from both these curves that the dielectric loss tangent increases rapidly for this material as the firing temperature is raised above 1100°C, and is quite high at 1250°C, the optimum firing temperature for both good alignment and high density. Thus some compromise must be sought between the loss tangent and the alignment and density requirements on firing temperature.

One possible cause for this rapid increase in loss tangent with firing temperature is that zinc is being lost on firing at the higher temperatures, and as a result the material has excess iron. It was to correct this possible cause that the iron deficient compositions were synthesized. It is seen particularly clearly in Figure 7 that the reduction in iron stoichiometry does, in fact, reduce the dielectric loss tangent in the final material. The lowest loss tangent measured, however, is still

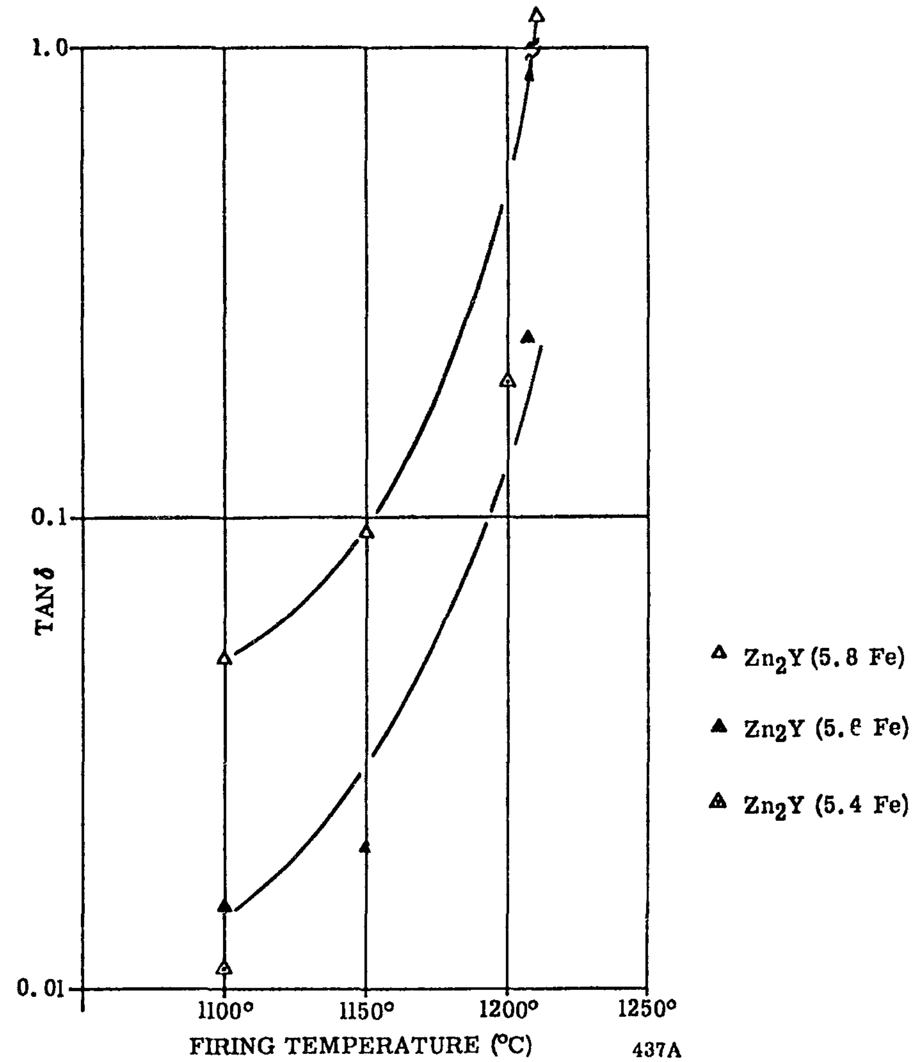

Figure 7. Dielectric loss tangent of Zn_2Y samples plotted as a function of firing temperature. Data shown were obtained by X-band cavity measurements and represent results obtained on materials of three different iron stoichiometries.

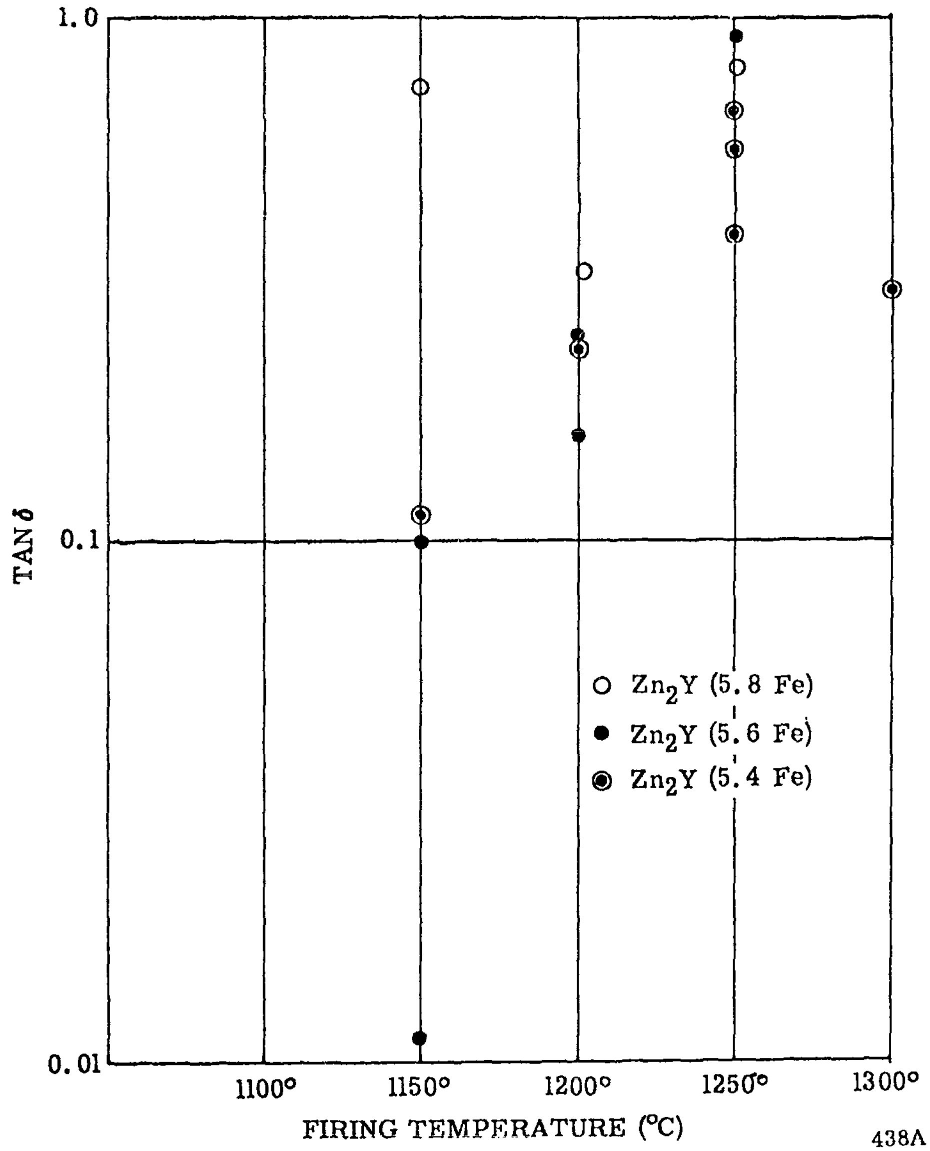

Figure 8. Dielectric loss tangent of Zn_2Y samples plotted as a function of firing temperature. Data shown were obtained from Q meter measurements at 20 Mc and represent results obtained on materials of three different iron stoichiometries.

0.011 - a relatively high value for microwave applications.

Figure 9 shows the dielectric loss tangent of the $Ni_{.3}Cu_{.7}Zn_{1.0}Y$ compound as a function of firing temperature. Data on two compositions of differing iron stoichiometry are also shown. These data, though not yet complete, indicate that iron stoichiometry is of little importance in determining the dielectric loss of these materials. These data were all taken at X-band by cavity perturbation techniques.

In Figure 10 are shown data taken by both cavity and Q meter methods on the $Cu_{.5}Zn_{1.5}Y$ compound.

It should also be noticed that in neither of these materials is there as strong a tendency for the dielectric loss to increase with increasing firing temperature as was experienced with the Zn_2Y. In fact, the dielectric loss of these compositions remain relatively constant as the firing temperature is raised to 1200°. At still higher firing temperatures there is some evidence of an increase in dielectric loss. The relatively flat curve of loss tangent as a function of firing temperature for these materials and the absence of any apparent dependence on iron stoichiometry both indicate that the loss of zinc is not severe with these two materials. Again loss tangents of the order of .01 to .02 are obtained.

Table I contains a variety of data on scattered, though representative, samples of planar materials. The data shown here illustrate the results obtained in terms of average values as well as departures from the average values. While some results may seem inconsistent from one standpoint or another, they are shown here nevertheless. The various samples were prepared with alcohol, Kyso 45 and water as a carrier in the attritor stage, and were fired at differing firing temperatures.

The saturation magnetization for the Zn_2Y material shown in Column 5 of this table is centered around approximately 2100 gauss with approximately 100

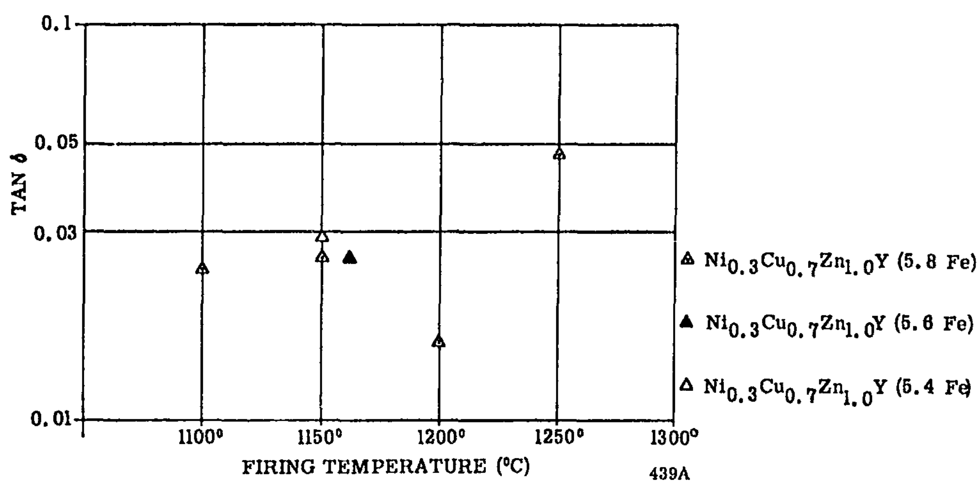

Figure 9. Dielectric loss tangent of $Ni_{0.3}Cu_{0.7}Zn_{1.0}Y$ samples plotted as a function of firing temperature. Data shown were obtained from X-band cavity measurements and represent results obtained on materials of three different iron stoichiometries.

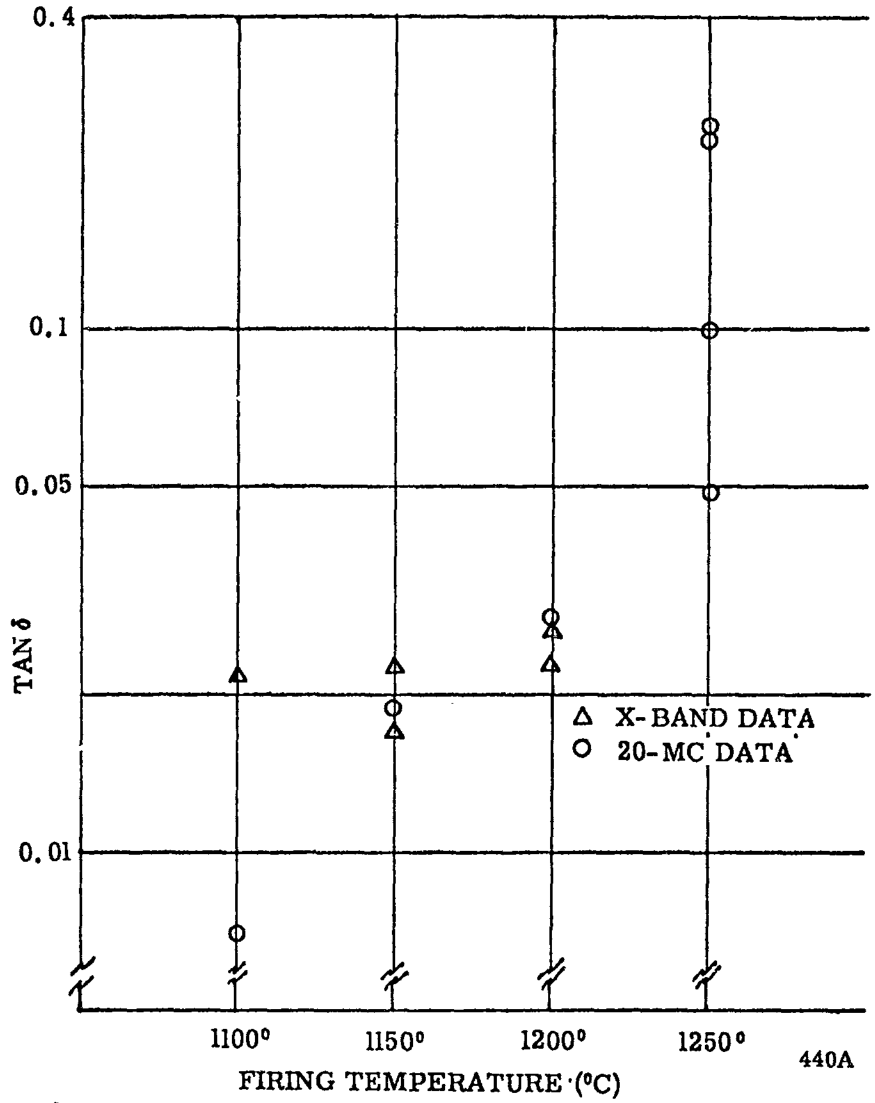

Figure 10. Dielectric loss tangent of $Cu_{0.5}Zn_{1.5}Y$ samples as a function of firing temperature. Data obtained from both X-band cavity measurements and 20 Mc Q meter measurements are shown on this graph.

TABLE I

1	2	3	4	5	6	7	8	9	10
No. Sample	Material	Firing Temperature (°C)	Carrier	$4\pi M_s$ (gauss)	F	ΔH (oe)	γ	H_{anis} 1 (oe)	H_{anis} 2 (oe)
HP-29A	$Zn_{2.0}Y$	1150	Alcohol	2180	.817	569		14,650	11,300
HP-29AX	$Zn_{2.0}Y$	1150	Alcohol	2090	.742	587			
HP-15A	$Zn_{2.0}Y$	1150	Kyso 45	2010	.18				
HP-15E	$Zn_{2.0}Y$	1200	Kyso 45	2180	.48	688	3.12	14,800	
HP-15C	$Zn_{2.0}Y$	1250	Kyso 45	2220	.605	589			15,000
HP-1C	$Zn\ \ Y$	1250	Water	2200	.347	1200			
HP-20B	$Cu_{.5}Zn_{1.5}Y$	1100	Alcohol	2260	.70	723			
HP-20A	$Cu_{.5}Zn_{1.5}Y$	1150	Alcohol	2320	.85	513	2.6	11,000	9,400
HP-20b	$Cu_{.5}Zn_{1.5}Y$	1200	Alcohol	2390	.995	496	2.14	21,677	12,400
HP-20F	$Cu_{.5}Zn_{1.5}Y$	1250	Alcohol	2370	.983	527	1.75	39,700	14,900
HP-19A	$Cu_{.5}Zn_{1.5}Y$	1200	Kyso 45	2260	.66	620			12,300
HP-19C	$Cu_{.5}Zn_{1.5}Y$	1200	Kyso 45	2000	.864	710	2.48	14,100	
HP-19E	$Cu_{.5}Zn_{1.5}Y$	1250	Kyso 45	2190	.713	682	1.96	18,700	13,600
HP-5A	$Cu_{.5}Zn_{1.5}Y$	1250	Water	2290	.792	1000			12,500
HP-21B	$Ni_{.3}Cu_{.7}Zn_{1.0}Y$	1100	Alcohol	2760	.601	419	2.61	9,200	8,600
HP-21A	$Ni_{.3}Cu_{.7}Zn_{1.0}Y$	1150	Alcohol	2330	.893	375	2.9	7,400	7,700
HP-21C	$Ni_{.3}Cu_{.7}Zn_{1.0}Y$	1200	Alcohol	2550	.984	431	2.46	13,700	10,700
HP-6A	$Ni_{.3}Cu_{.7}Zn_{1.0}Y$	1250	Water	2820	.358				
HP-21A	$Ni_{.3}Cu_{.7}Zn_{1.0}Y$(5% Al)	1150	Alcohol	1530	.232	435		7,094	7,213
HP-21C	$Ni_{.3}Cu_{.7}Zn_{1.0}Y$(5% Al)	1200	Alcohol	1590	.476	400		7,700	7,660
HP-7D	$Ni_{.3}Cu_{.7}Zn_{1.0}Y$(5% Al)	1250	Water	2400	.6	870		8,430	
HP-8B	$Ni_{.3}Cu_{.7}Zn_{1.0}Y$(10% Al)	1250	Water	2450	.284	1800		750	
HP-8A	$Ni_{.3}Cu_{.7}Zn_{1.0}Y$(10% Al)	1250	Water	2130		1400		1,000	
HP-9A	$Ni_{.3}Cu_{.7}Zn_{1.0}Y$(15% Al)	1250	Water	2490					
HP-4	$Ni_{1.0}Zn_{1.0}Y$	1250	Water	2390	.863	1000		13,600	
HP-18	$Ni_{1.0}Zn_{1.0}Y$	1250	Kyso 45	2450	.434	680		15,000	
HP-12E	$Co_{2/3}Cu_{2/3}Zn_{2/3}$	1150	Kyso 45	2219	.24				
OG-5	$3Y_2O_3 \cdot 5Fe_2O_3$	1450	Alcohol			18.3			

gauss spread in measured values. Data on the $Cu_{.5}Zn_{1.5}Y$ compounds indicate a saturation magnetization near 2300 gauss. In this case the spread of data is somewhat greater, and on one sample a value of only 2000 gauss was measured. The $Ni_{.3}Cu_{.7}Zn_{1.0}Y$ compound has a saturation magnetization of approximately 2550 gauss. The data on the aluminum substituted nickel-copper-zinc compound show rather erratic results for the 5 percent aluminum substituted compound. On the other hand, no significant change in magnetization occurs when 10 and 15 percent aluminum is substituted for iron. X-ray diffraction data strongly indicated a second phase formation as evidenced here by the small alignment factors.

Column 7 of Table I lists measured values of linewidth on the different compositions as a function of firing temperature and carrier used. It should be evident from this data that in most instances the measured linewidth bears an inverse relation to the alignment index. Misalignment seems to be the chief cause of line broadening in those compounds with single phases present. Narrowest linewidths are obtained on the $Ni_{.3}Cu_{.7}Zn_{1.0}$ Y material but the smallest value measured to date is still approximately 375 oersteds. In view of the extremely high values of alignment index achieved and the relatively high density of these samples it is difficult to understand the reason for this broad linewidth. Different compositions will be tried in the vicinity of this compound in order to see if a departure from this chemical formula will result in a more narrow linewidth. In addition, efforts will be made to determine whether or not the measured linewidth varies with orientation of the r-f magnetic field. Measured linewidths are found to vary by as much as 20 percent between measurements taken on samples of the same material at X- and V-band frequencies. No consistent frequency dependence is presently noted.

Columns 8, 9, and 10 contain g-factor and anisotropy field data for several different compositions. The values listed in Columns 8 and 9 are deduced from

resonance measurements at X- and V-band frequencies as outlined in Section 2.3. Values listed in Column 10 are computed from X-band measurements alone under the assumption that $g = 2$ or $\gamma = 2.8$. It should be pointed out that the computations involved in determining those values listed in Columns 8 and 9 are rather sensitive to small errors in determining the field required for resonance at the two frequencies.

Because of the extremely good alignment factors achieved on planar materials, effort was carried out on an associated company-sponsored program to test these same methods on cubic materials. Listed at the bottom of Table I is the linewidth determined on a single sample of polycrystalline yttrium iron garnet that was pressed using the orientation techniques evolved in this study of planar materials. The density can be considerably improved by employing a different firing temperature. The fact that a linewidth of only 18.3 oersteds was obtained on this polycrystalline material with relatively low density is felt to be a good indication of at least partially successful alignment of the cubic grains of this material. Unoriented polycrystalline garnet materials having the same densities normally show linewidths of the order of 60 oersteds so that a marked reduction has been achieved. Because of the important practical implications of this result, this effort is being continued into the next quarter. If it does prove feasible to orient the grains of cubic garnets and ferrites and thereby drastically reduce their linewidths, a whole new generation of magnetic materials would be available.

3.5 APPLICATIONS STUDIES

During the past quarter studies have been initiated into the application of planar materials to practical microwave devices. Initial efforts have been concentrated on possible isolator configurations.

c. Theoretical Analysis

It is perhaps well known[1] that the maximum isolation ratio of a magnetic material located in a waveguide is given by perturbation theory as

$$F_{max} = \frac{(\chi_{xx}'' \chi_{zz}'')^{\frac{1}{2}} + \chi_{xz}''}{(\chi_{xx}'' \chi_{zz}'')^{\frac{1}{2}} - \chi_{xz}''}, \tag{3}$$

when one assumes the dielectric losses are not comparable to the magnetic losses. χ_{xx}'', χ_{zz}'', and χ_{xz}'' are the appropriate terms of the susceptibility tensor and the d-c magnetic field is considered applied in the y-direction . By using susceptibility terms appropriate to the particular case of planar ferrites one can determine the optimum material configuration as well as the influence of various material properties on this maximum isolation ratio.

The susceptibility terms can be derived from the Landau-Lifshitz equation

$$\frac{d\vec{M}}{dt} = \gamma \vec{M} \times \vec{H} + \frac{\alpha \gamma}{M_s} \vec{M} \times \vec{M} \times \vec{H}, \tag{4}$$

where M, H, and γ are as previously defined, and α is the appropriate damping factor. Following through the derivation for a planar material with easy plane in the x-y plane, one finds for the imaginary or loss terms of the tensor susceptibility

$$\chi_{xx}'' = \frac{4\pi M_s}{D} \alpha H_i \left[H_x^2(1 + \alpha^2) + H_i^2\right] \tag{5}$$

$$\chi_{zz}'' = \frac{4\pi M_s}{D} \alpha H_i \left[H_z^2(1 + \alpha^2) + H_i^2\right] \tag{6}$$

and

$$\chi_{xz}'' = \frac{4\pi M_s}{D} \alpha H_i^2 \left\{H_z + H_x\right\}, \tag{7}$$

where

$$H_z = H_o + M_s (N_x - N_y)$$

$$H_x = H_o + H_A + M_s(N_z - N_y),$$

$$H_i = \frac{\omega}{|\gamma|},$$

and

$$D = \left[H_x H_z (1 + \alpha^2) - H_i^2\right]^2 + \alpha^2 H_i^2 (H_x + H_z)^2.$$

By inserting equations (5), (6), and (7) into (3) and assuming that F_{max} occurs at resonance, that is

$$H_i^2 = H_x H_z,$$

and further that

$$\alpha^2 \ll 1,$$

the relation for F_{max} becomes

$$F_{max} = \frac{4}{\alpha^2}, \tag{8}$$

and since $\alpha = \frac{\gamma \Delta H}{2\omega_r}$ this becomes the familiar relation

$$F_{max} = \left(\frac{4\omega_r}{\omega_{\Delta H}}\right)^2. \tag{9}$$

The relationship for the maximum isolation ratio indicates that this ratio is independent of the anisotropy field of the material.

It is to be noted that equations (3) through (9) were derived assuming the applied field, H_o, is sufficient to saturate the material. The required applied field for resonance may be determined from the equation of resonance for a planar hexagonal material,

$$\omega = \gamma \left[H_o + H_A + (N_z - N_y)M_s\right] \left[H_o + (N_x - N_y)M_s\right]^{1/2},$$

where the x-y plane is the easy plane of the material, and the y-direction corresponds to the direction of the applied field, H_o. It may be shown, that the field required for resonance in a given configuration may not always be sufficient for saturation.

Consider as typical examples of waveguide geometries those shown in Figure 11. Assigning parameter values of

$$H_A = 10 \times 10^3 \text{ oersteds,}$$

$$4\pi M_s = 2.4 \times 10^3 \text{ oersteds,}$$

$$\gamma = 2.8 \text{ Mc/oersted,}$$

and $$\omega = 3 \text{ Kmc .}$$

We find the following results for a slab with dimensions .875" x .125" x .020".

CASE I - for the easy plane parallel to the plane of the slab and the slab normal to the broadwall of the waveguide, the required H_o is 400 oersteds.

CASE II - for the easy plane perpendicular to the plane of the slab and the slab normal to the broadwall of the waveguide, the required H_o is 1600 oersteds.

CASE III - for the easy plane longitudinal to the waveguide axis and the slab parallel to the broadwall of the waveguide, the required H_o is 3700 oersteds.

CASE IV - for the easy plane transverse to the waveguide axis and the slab parallel to the broadwall of the waveguide, the required H_o is 1810 oersteds.

In Cases I and II the demagnetizing field is 336 oersteds and in Cases III and IV the demagnetizing field is 2020 oersteds. Thus it is seen that Case III would provide the greatest degree of saturation; however, it also requires the greatest applied field for resonance. Isolator measurements during this interim have been primarily confined to Cases I and III due to the size and shape of presently available planar material.

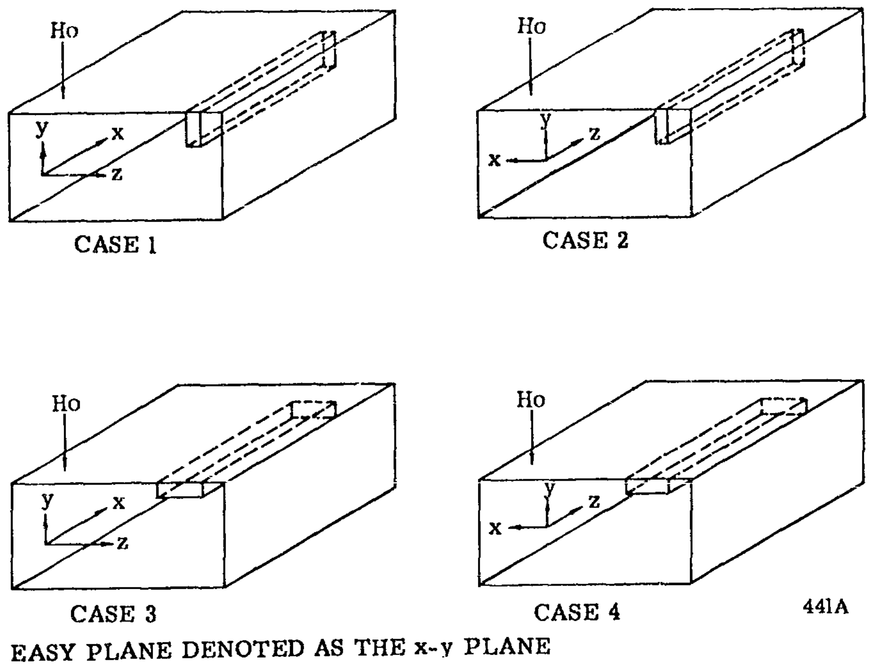

Figure 11. Various possible configurations of a planar material mounted in a rectangular waveguide.

b. Measurements on Isolator Configurations

During this second quarter investigations were conducted to determine the performance of isolators using the best of the available planar hexagonal materials. The principle aim of this study was to determine the correlation between theoretical predictions and experimental results. The material investigated was $Ni_{.3}Cu_{.7}Zn_{1.0}Y$. The material was made into slabs and mounted on the broad wall of both S- and X-band rectangular waveguides and subsequently inserted in a variable magnetic field. A special section of waveguide was designed with one broad wall in the form of a sliding plate, so that the position of the ferrite could be continuously varied within the waveguide.

A slab of $Ni_{.3}Cu_{.7}Zn_{1.0}Y$ material fired at 1150°C was mounted on the broad wall of the waveguide as shown in Figure 11, Case III. The dimensions were .94" x .125" x .032". The response of the isolator to a varying applied d-c magnetic field at a frequency of 9 Kmc was observed for different positions of the ferrite across the broad wall of the waveguide. These curves of attenuation versus applied field are seen in Figure 12. Figure 13 shows isolation ratios measured at resonance versus the position of the ferrite across the waveguide. It can be noted that the maximum isolation ratio is obtained with the slab positioned one quarter of the broad dimension across the waveguide. Theoretical calculations[2] show that for maximum isolation ratio for the given material, the ratio of the magnetic fields, $\frac{h_z}{h_x}$, should be 3.78 to 1. This corresponds to a position across the waveguide of .435 of the total width at the measurement frequency. The zero db reference

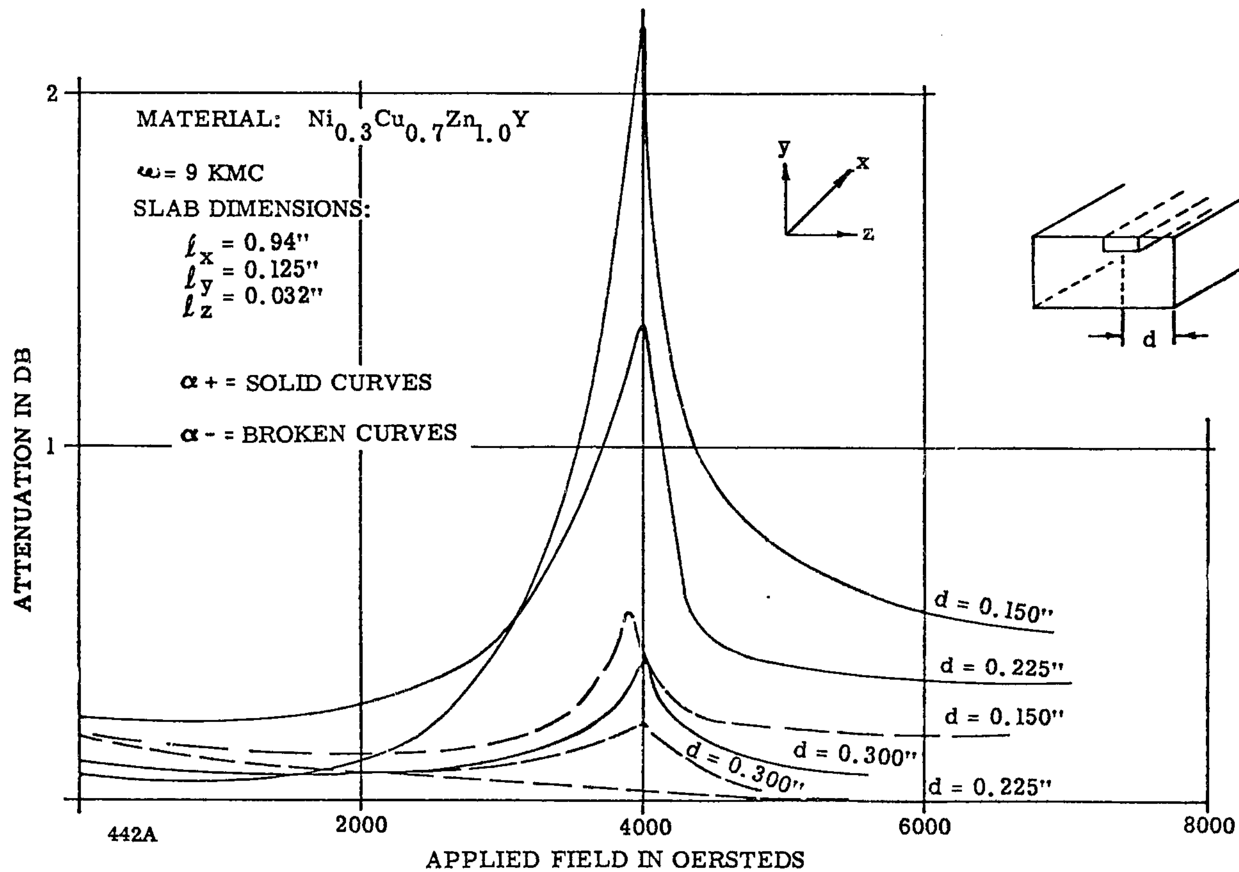

Figure 12. Curves of forward and reverse attenuation measured as a function of applied field for a slab of $Ni_{0.3}Cu_{0.7}Zn_{1.0}Y$ materials in the configuration of Case 3 of Figure 11. The parameter in these curves is the position of the slab across the broadwall of the waveguide.

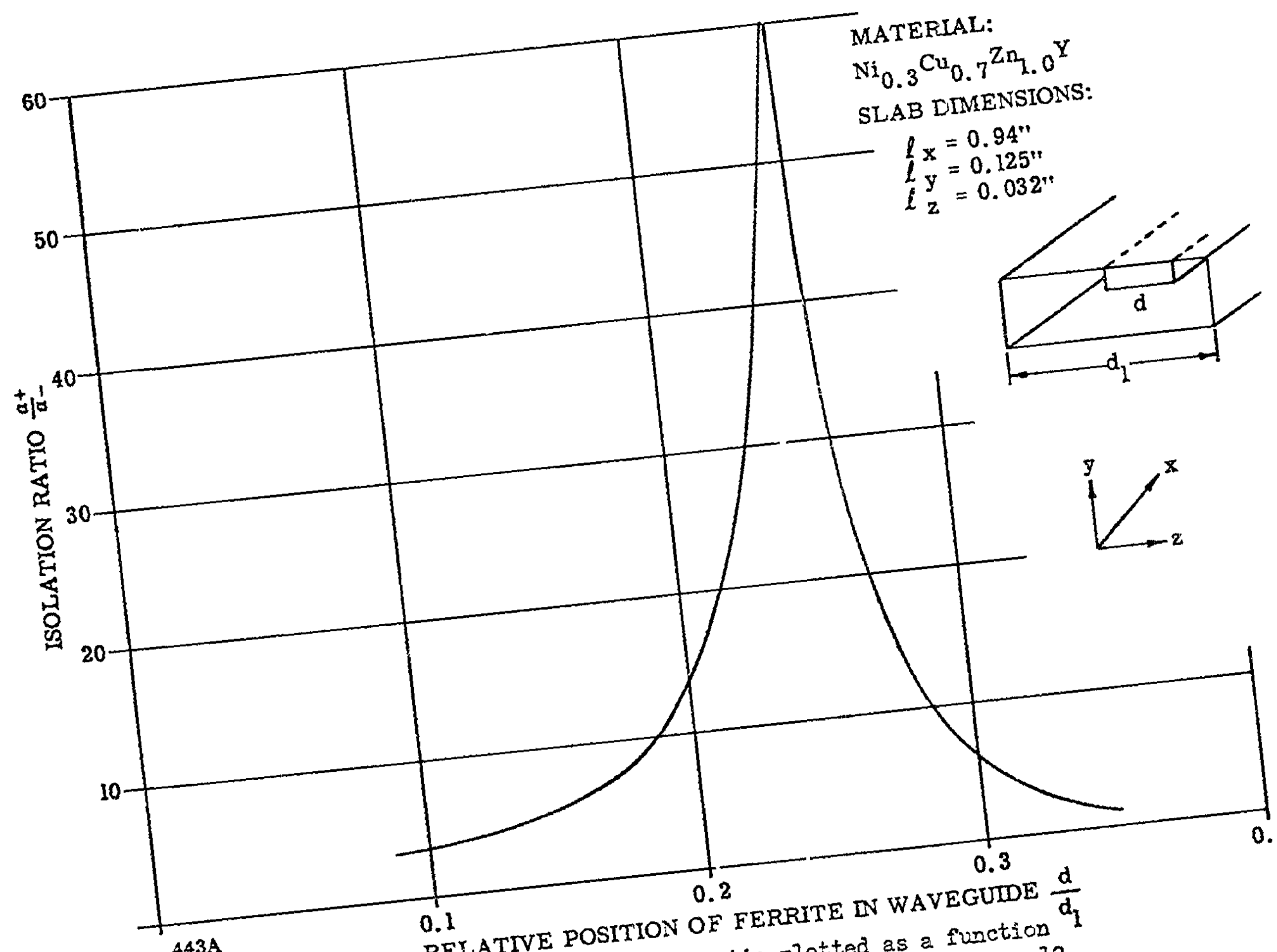

Figure 13. Measured values of isolation ratio plotted as a function of the relative position of the ferrite slab of Figure 12 across the broadwall of the waveguide.

level for these attenuation curves and isolation ratios was taken as the output reading obtained with a maximum field applied in the low loss direction. Hence, any dielectric losses associated with the slab being measured are not considered in determining these isolation ratios, and will degrade actual performance. The size and shape of planar ferrites now available limits the dimensions of the slabs and restricts isolation values of a single slab to small values.

The same material was made into a slab of dimensions .035" x .25" x .875" and mounted in the waveguide in accordance with Figure 1, Case I. Measurements were carried out at 10 Kmc and the response of the isolator to the applied field is seen in Figure 14. Figure 15 shows isolation ratios at resonance versus the relative position of the ferrite within the waveguide.

Additional isolator measurements were taken at S-band with larger slab sizes. The isolation ratios obtained were relatively low and this is believed to be caused by incomplete saturation of the material. To effectively construct isolators using these planar materials at the lower frequencies one must determine a technique of lowering either the anisotropy field, the $4\pi M_s$ value, or perhaps both.

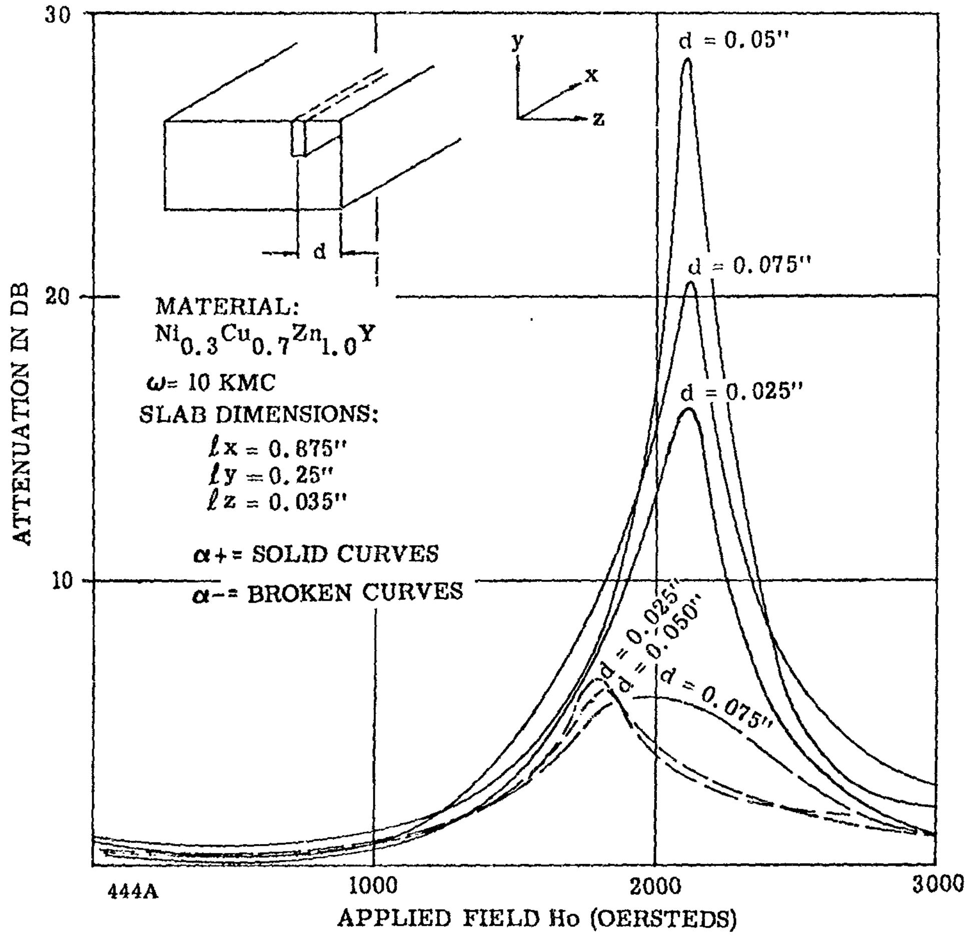

Figure 14. Curves of forward and reverse attenuation measured as a function of applied field for a slab of $Ni_{0.3}Cu_{0.7}Zn_{1.0}Y$ materials in the configuration of Case 1 of Figure 11. The parameter in these curves is the position of the slab across the broadwall of the waveguide.

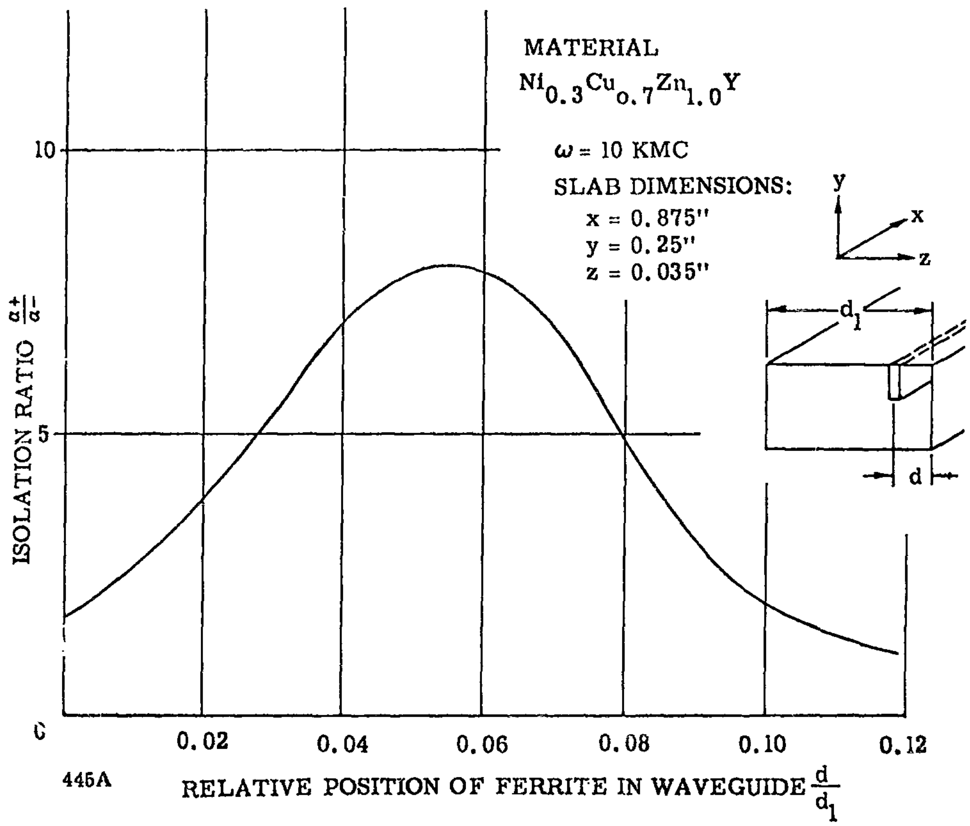

Figure 15. Measured values of isolation ratio plotted as a function of the relative position of the ferrite slab of Figure 14 across the broadwall of the waveguide.

4. CONCLUSIONS

The preparation process evolved is capable of producing good ceramic materials with high density and good alignment. These materials do not as yet exhibit as narrow a linewidth as expected. Compositions near those already tried should be checked out. Trivalent aluminum substituted for trivalent iron apparently forms a second phase material rather than entering the Y structure. A deficiency of iron helps to lower the dielectric loss tangent of Zn_2Y, perhaps by offsetting the zinc loss on firing, but this step is not universally effective among the other Y compounds.

By using the alignment techniques developed for these planar materials, cubic ferrites can be successfully oriented even in cases of small anisotropy. At least partially successful alignment has been achieved on yttrium iron garnet wit anisotropy fields of 40 oersteds.

While initial isolator measurements are encouraging, the fabrication of practical low frequency isolators will require improved materials in terms of linewidth, and larger sized samples.

5. PROGRAM FOR NEXT INTERVAL

The materials effort for the next quarter will concentrate on the study of compounds with compositions near $Ni_{.3}Cu_{.7}Zn_{1.0}Y$, $Ni_{1.0}Zn_{1.0}Y$, and $Cu_{0.5}Zn_{1.5}Y$ in an effort to obtain materials with improved linewidths. The process now used seems adequate to produce materials of good ceramic quality and alignment. Effort will be made to procure pressing equipment capable of preparing samples of larger physical dimensions.

Some studies of oriented cubic materials will be continued as a natural extension of the materials effort specified in this contract.

Studies of isolator performance utilizing planar hexagonal ferrites will be continued during the next quarter. The configurations with the easy plane transverse to the waveguide axis, Cases II and IV of Figure 11, will be investigated and compared to Cases I and III. The results obtained empirically and that expected through theoretical predictions will be analyzed. A final analysis of some of the inherent advantages or disadvantages of each of the configurations will be made.

The features of using the planar hexagonal materials in a coaxial structure will be analyzed and measurements of isolator performance within these internal magnet structures will be made. However, in considering a configuration for proposed isolator design, the feature of high power handling capabilities will be of primary consideration.

The utilization of dielectric materials for optimizing the performance of isolators employing the planar hexagonal materials will be investigated, also the degree of degradation of isolator performance produced by the dielectric losses within the planar materials will be determined.

During the next interim the analysis and development of a microwave switch operated by the planar hexagonal materials will commence.

UNCLASSIFIED

UNCLASSIFIED